



## Surface contamination of single-crystal PuSb

S.R. Wasserman<sup>a,\*</sup>, L. Soderholm<sup>a</sup>, J. Rebizant<sup>b</sup>, G.H. Lander<sup>b</sup>

<sup>a</sup>Chemistry Division, Argonne National Laboratory, 9700 S. Cass Ave., Argonne, IL 60439, USA

<sup>b</sup>European Commission, JRC, Institute for Transuranium Elements, Postfach 2340, D-76125, Karlsruhe, Germany

### Abstract

Pu M-edge X-ray absorption experiments were performed on a single crystal of PuSb in order to understand incongruous X-ray resonant exchange scattering (XRES) results from the same material. Analysis of the extended X-ray absorption fine structure (EXAFS) reveals that there is an amorphous or polycrystalline surface phase on the PuSb. The Pu at the surface of the crystal is coordinated primarily to a first-row main-group element, probably oxygen. In addition, the surface may be slightly deficient in antimony. These EXAFS results are sufficient to explain the absence of an XRES response in this PuSb sample. © 1998 Elsevier Science S.A.

*Keywords:* X-ray resonant exchange scattering; X-ray absorption fine structure; Surface contamination; PuSb

### 1. Introduction

The magnetic properties of actinide pnictides have long been of interest [1]. Recently, efforts to further quantify the magnetic properties of these materials have utilized X-ray resonant exchange scattering (XRES) [2–4]. However, experiments designed to compare XRES results from crystals of NpS and PuSb and a thin film of UPd<sub>2</sub>Al<sub>3</sub> have produced rather incongruous results. Whereas significant magnetic scattering was observed from the U and Np compounds, there was no detectable magnetic response from the Pu analog. The latter result contrasts with calculations that show the Pu in PuSb to have a moment sufficient to produce observable scattering [5]. These XRES experiments raised the question of whether fundamental physics plays a role in the anomalous results for PuSb, or whether there was an experimental complication. In order to understand the absence of an observable magnetic response in the XRES measurements on PuSb, the intensities of the (002) reflection from each sample were monitored as the energy was scanned through a range that encompassed the M<sub>5</sub> and M<sub>4</sub> X-ray absorption edges of each of the actinides. In principal, this experimental configuration should measure the diffraction anomalous fine structure (DAFS) [6]. In the case of PuSb, the range in energy also included the Sb L<sub>3</sub> absorption edge. The latter experiments were performed at room temperature, which is well above the magnetic ordering temperature of T<sub>N</sub>=85 K

reported for PuSb [1]. Because PuSb has the NaCl structure (Fm3m), the (002) reflection has contributions from all atoms in phase and corresponds to the scattering factor f(000). The results from these experiments on PuSb and their implications are presented herein.

### 2. Experimental

The <sup>239</sup>PuSb single crystal, with dimensions of approximately 1.5×1.5×0.3 mm, was grown at the Institute for Transuranium Elements, Karlsruhe. The sample was encapsulated in a copper holder with thin (0.2 mm) beryllium windows. The X-ray scattering experiments were performed at beamline X22C at the National Synchrotron Light Source (NSLS). The measurements were executed at room temperature. The scattering was monitored by scanning the monochromator and monitoring the (002) peak intensity. Corrections for the beryllium and Kapton in the X-ray beam, total thicknesses of 1.7 mm and 0.28 mm, respectively, have been applied to the data.

### 3. Results and discussion

#### 3.1. Data reduction

The intensity of the PuSb (002) reflection as a function of the X-ray energy is compared with analogous data from UPd<sub>2</sub>Al<sub>3</sub> and NpS in Fig. 1. The observed intensities are

\*Corresponding author. Tel.: (1-630) 252-3527; fax: (1-630) 252-4225; e-mail: srw@anl.gov

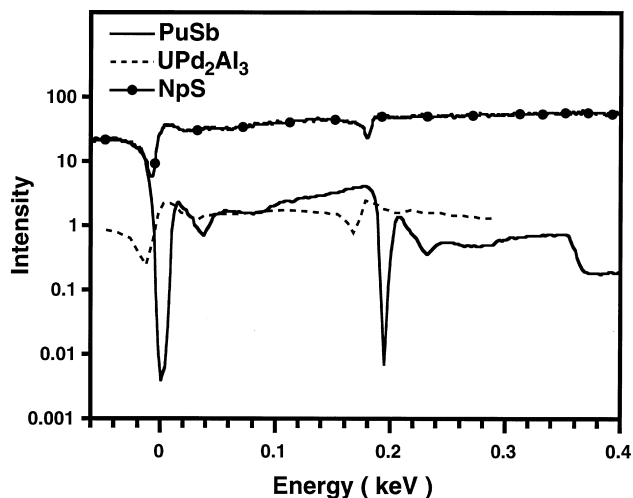


Fig. 1. Intensity of the (002) reflection as a function of energy for a thin film of  $\text{UPd}_2\text{Al}_3$ , neptunium sulfide (NpS), and plutonium antimonide (PuSb). The energy scale is relative to the standard threshold energy for the  $M_5$  absorption edge of each element.

proportional to the total scattering factor, which can be expressed as:

$$f = f_0 + f' + if'' \quad (1)$$

The  $f_0$  term represents the nonresonant charge scattering. The  $f' + if''$  terms represent the resonant, dispersive contributions that change with energy, and correspond to the anomalous scattering and absorption, respectively. Unlike the U and Np data, the Pu absorption does not return to 'baseline' at energies higher than the absorption edge. This feature of the data indicates a dominant contribution from the absorption  $f''$  term, suggesting that this experiment may simply measure absorption by the sample. This fact, combined with the significantly reduced Bragg scattering at resonance from the PuSb crystal compared to the intensities observed from the Np and U samples (Fig. 1) leads us to suspect that there is an amorphous or polycrystalline phase on the surface of the sample. The combination of low X-ray energies ( $\approx 3.8$  keV) needed for resonant experiments at the Pu M edges, the intrinsic heavy-atom absorption, and the experimental geometry combine to give a sampling depth of only about  $0.4 \mu\text{m}$ . In other words, only the top  $0.4 \mu\text{m}$  of the sample is influencing the data.

The oscillations in the observed intensity at X-ray energies greater than the edges (Fig. 1), which are most prominent for the PuSb data, result from an interference pattern set up by the central ion's outgoing photoelectron as it is reflected back by the neighboring ions. The presence of an amorphous or polycrystalline phase on the surface has implications for the interpretation of the data from PuSb. Whereas the experimental geometry dictates that the data should be treated as DAFS data, the spectrum may instead represent standard extended X-ray absorption

fine structure (EXAFS). Our examination of the PuSb data indicate that they are well represented by a standard EXAFS analysis. This conclusion supports our hypothesis that there is a contamination layer on the surface of the single crystal of PuSb that is contributing significantly to the data shown in Fig. 1.

### 3.2. Data analysis

We have followed the general methods for the analysis of EXAFS data [7] in order to examine the surface composition of the PuSb crystal. The Pu EXAFS data from both the  $M_5$  and  $M_4$  edges, obtained by subtracting the background contributions from the nonresonant terms in Eq. (1), are plotted in Fig. 2. The energy scale has been converted to  $k$ -space using Eq. (2), where  $k$  is the electron wavevector, and  $(E - E_0)$  is the

$$k = 0.5123(E - E_0)^{1/2} \quad (2)$$

difference in energy between the incoming X-ray beam and the threshold energy for emission of a photoelectron from the absorbing atom [8]. The Fourier transform of the

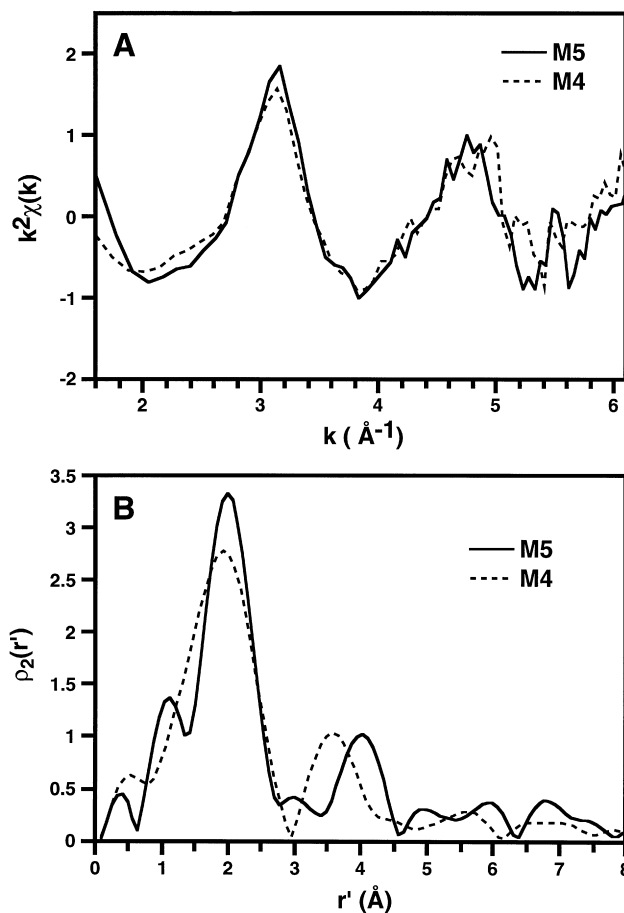


Fig. 2. Extended X-ray Absorption Fine Structure for the  $M_5$  (solid line) and  $M_4$  (dashed line) edges of PuSb: (A)  $k^2$ -weighted EXAFS; and (B) radial structure functions.

EXAFS as a function of  $k$  represents the local structure around the absorbing atom. Fig. 2 also includes these radial structure functions. We have used  $k^2$  rather than  $k^3$  weighting of the data in these transforms in order to minimize artifacts due to noise in the original data. The overall similarity of the EXAFS from the two edges transfers directly to the radial distributions.

The features in the transformed functions are rather broad, a result of the limited  $k$ -range of EXAFS data. The presence of the  $M_4$  edge of Pu limits the EXAFS from the  $M_5$  edge to approximately  $6.5 \text{ \AA}^{-1}$ . Similarly, the  $L_3$  edge from antimony restricts the EXAFS range from the  $M_4$  edge. In Fig. 2 the ranges for the Fourier transforms extended from 1.6 to  $6.5 \text{ \AA}^{-1}$  for the  $M_5$  edge and from 1.6 to  $6.1 \text{ \AA}^{-1}$  for the  $M_4$ . (Normally, a  $k$  range of approximately  $2\text{--}12 \text{ \AA}^{-1}$  permits a complete analysis of the local structure about the absorbing ion.) The radial structure functions are dominated by the first coordination shell of plutonium. Since the other features in the radial structure functions do not correspond in the data from the two edges, they are probably due to the high level of noise in the data. Despite the limited energy range and quality of the data under consideration here, the transforms do suggest that plutonium is not in a well ordered environment.

The Fourier-transformed radial-distribution functions, reported as a function of  $r'$ , do not include corrections to account for the phase changes of the photoelectron that arise during the scattering process. These phase corrections have contributions from both the central ion and the surrounding ligands and are element specific. Typically the peaks in an uncorrected radial-structure function appear at approximately  $0.3 \text{ \AA}$  less than the true bond distance. The centroid of the main peak in the Fourier transforms shown in the figure is at  $2.0 \text{ \AA}$ , suggesting that the nearest neighbor(s) to plutonium are at about  $2.3 \text{ \AA}$ , a distance incompatible with a Pu–Sb interaction. In crystals of PuSb, the bond distance between the two elements is  $3.12 \text{ \AA}$  [9] whereas in crystalline PuO<sub>2</sub>, the Pu–O distance is  $2.33 \text{ \AA}$  [10]. The uncorrected radial distributions obtained from the PuSb sample are more consistent with a Pu–O interaction than with a Pu–Sb interaction.

Following standard practice in EXAFS analysis, we have determined approximate structural parameters from the Fourier-filtered EXAFS of the first coordination shell. This procedure requires the inclusion of the scattering amplitudes and the phases that were not necessary to determine the radial structure functions of Fig. 2. We have used theoretical single scattering phase shifts and amplitudes for M edges calculated by Feff 7 [11]. The best fit to the data using Pu–O gave a bond distance of  $2.29 \text{ \AA}$ , which corresponds well to the  $2.33$  expected for the oxide. When scattering parameters for PuSb were used, the fit results were physically unreasonable. Since the antimonide crystal was exposed to nitrogen during its synthesis, we also considered the possibility of the formation of PuN. When parameters for this compound were used in the

EXAFS analysis, the fitted bond distance was within  $0.01 \text{ \AA}$  of that found for the oxide. This result is reasonable, since scattering of a photoelectron by nitrogen and oxygen is similar. In fact, EXAFS cannot normally distinguish between coordination shells composed of oxygen, nitrogen or other first-row elements. However, the bond distance in crystalline PuN is  $2.45 \text{ \AA}$  [10]. Since both the Pu–O and Pu–N reference data give bond distances on the order of  $2.3 \text{ \AA}$ , the surface contaminant is probably the oxide, rather than the nitride.

In order to confirm that EXAFS can easily distinguish between PuSb and PuO<sub>2</sub>, we have modeled the expected radial structure functions of PuO<sub>2</sub>, PuSb and PuN using multiple scattering EXAFS calculations from Feff 7. The results of these calculations are compared with the observed coordinative distribution in Fig. 3. These calculations utilize the geometries found in the crystalline versions of these compounds. Two user-adjustable parameters were included: one to reflect Debye-Waller type disorder, the other to correct for differences in the energy reference

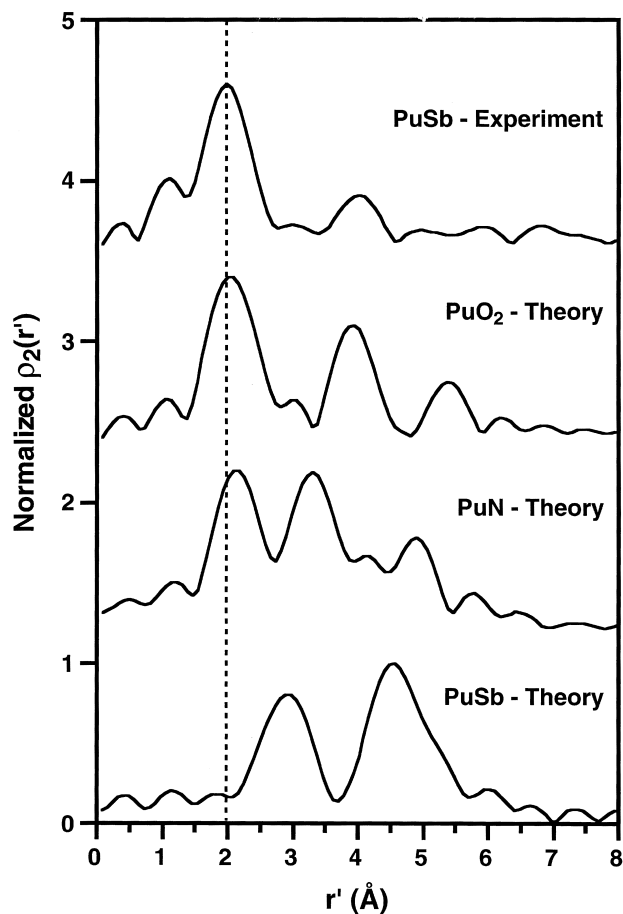


Fig. 3. Comparison of the radial structure function from the  $M_5$  edge of PuSb with simulations of the radial distributions expected for crystalline PuO<sub>2</sub>, PuN and PuSb. The Fourier transforms of the experimental and simulated  $k^2$ -weighted EXAFS data extended in the range  $\Delta k = 1.6\text{--}6.5 \text{ \AA}^{-1}$ . The maxima in each distribution are normalized to 1. The offset between successive structure functions is 1.2.

level between the experimental data and the calculation. The position of the first coordination shell does not agree with that expected for PuSb. The agreement between the experimental data and the PuO<sub>2</sub> model is good, although as previously stated it is apparent that the sample does not possess significant long-range order.

Whereas it is clear that there is a surface layer on the crystal that is different from PuSb, it is difficult to assess its origin. The syntheses and most experiments on PuSb are performed under an inert atmosphere [12]. Our results show that the Pu at the surface is coordinated primarily to a first row main group element, probably oxygen, although an oxy-carbide, similar to that reported on the surface of oxide-coated Pu metal which has been heated under vacuum [13], cannot be ruled out. Contamination may have occurred during the initial formation of the compound. Alternatively, radiation damage induced by the <sup>239</sup>Pu of the glue holding the crystal in place may have resulted in chemical reactions at the surface and degradation of the material. The latter hypothesis may explain why a surface contaminant was observed on the PuSb crystal, but not the USb [2]. Whereas thermodynamic data are not available for plutonium antimonide, the enthalpy of formation for the corresponding uranium compound is  $-33.1 \text{ kcal mol}^{-1}$  [14]. Since the heat of formation of uranium dioxide, UO<sub>2</sub>, is  $-260 \text{ kcal mol}^{-1}$  [15] and those of the common antimony oxides are also negative [16], the formation of UO<sub>2</sub> by oxidation of USb is thermodynamically favored. We may expect similar reactivity for PuSb.

### 3.3. $M_5$ versus $M_4$ edges

Although the EXAFS data from the  $M_5$  and  $M_4$  edges of plutonium are similar, there is one significant difference between the two spectra: the narrow feature that appears only in the  $M_5$ -edge data at  $5.5 \text{ \AA}^{-1}$ . This peak appears at roughly the position expected for the absorption edge of americium. However, the amount of Am expected in this sample is low, approximately 0.2% [4], and is probably too small to be detected in a transmission XAS experiment. In addition, if the feature were due to absorption from americium, it would be expected in both the  $M_5$  and  $M_4$  data, although the positions of the absorption maximum would be different in the two spectra. This difference would arise because the energy of the Pu  $M_5$  edge is approximately 109 eV lower than that of Am. The difference in energy between the  $M_4$  edges is about 10 eV less than that. The failure to observe a similar peak in the  $M_4$  edge suggests that what is observed in the  $M_5$  edge is an experimental artifact.

Another curious feature in both the  $M_5$  and  $M_4$  EXAFS spectra is the peak at  $3.1 \text{ \AA}^{-1}$ . Although it appears in the data from both edges, the shape and intensity of the EXAFS in this region are atypical of extended fine structure. Whereas the shape may well reflect the crude resolution of the data at low  $k$ , the intensity is considerably

greater than that expected for a single oxygen coordination shell. Similar intensities have been observed in the  $L_3$  edges of UO<sub>2</sub> and PuO<sub>2</sub>, where they have been attributed to  $\sigma$ -type shape resonances of the metal–ligand bond [17]. Significantly, such resonances are not observed for the antimonides of both uranium and plutonium. There is also the possibility that the intensity may reflect an anomalous contribution by  $f'$  to the detected absorption spectrum.  $f'$  has a negative slope in the energy region that corresponds to this wavevector, which may reinforce the maximum in the absorption spectrum (see Fig. 1). The limited data prevent an analysis of this possibility.

### 3.4. Pu:Sb ratio

Our analysis of the EXAFS signal from the PuSb crystal suggests that the plutonium at the surface is bound to oxygen. However, antimony is detected in these experiments. As the energy of the incoming X-ray is scanned through the  $L_3$  edge of antimony at 4132 eV, absorption due to that element appears (Fig. 1). We have compared the relative intensities of the Pu  $M_5$  and Sb  $L_3$  edges with that expected for pure PuSb. The observed intensity ratio for plutonium to antimony is at least 2.1. The calculated ratio, based on the McMaster coefficients [18], is 1.8, which may suggest that there is a slight excess of plutonium over antimony at the surface of the crystal. Although we can, in principle, analyze the EXAFS from the Sb edge, the data are not of sufficient quality to do so. Nevertheless, we can conclude that there is a mixture of chemical constituents at the surface of this material.

## 4. Conclusions

The failure to observe X-ray resonant exchange scattering during experiments on a <sup>239</sup>PuSb crystal has been explained by an analysis of absorption data taken as a function of energy. The low intensity of the (002) Bragg reflection at resonance, together with the shape of the intensity vs. energy spectra obtained about the  $M_5$  and  $M_4$  edges of Pu, indicate the presence of an amorphous layer of a Pu-containing compound on the surface of the crystal. The presence of surface contamination on the PuSb crystal is confirmed by an analysis of EXAFS data that show the Pu to be bound primarily to a first-row main-group element, probably oxygen. In addition, the ratio of Pu to Sb determined from the absorption data indicates that there is an excess of Pu over Sb.

## Acknowledgements

This research was supported by the Division of Chemical Sciences, Office of Basic Energy Sciences, US Department of Energy under contract no. W-31-109-ENG-38. Work at the National Synchrotron Light Source of

Brookhaven National Laboratory is supported by the US DOE under contract no. DE-AC02-76CH00016.

## References

- [1] K.A. Gschneider, L. Eyring, G.H. Lander, G. Choppin (Eds.), Handbook on the Physics and Chemistry of Rare Earths, Chaps. 114–117, Elsevier Science, Amsterdam, 1993.
- [2] C.C. Tang, W.G. Stirling, G.H. Lander, D. Gibbs, W. Herzog, P. Carra, B.T. Thole, K. Mattenberger, O. Vogt, Phys. Rev. B 46 (1992) 5287.
- [3] E.D. Isaacs, D.B. McWhan, C. Peters, G.E. Ice, D.P. Siddons, J.B. Hastings, C. Vettier, O. Vogt, Phys. Rev. Lett. 62 (1989) 1671–1674.
- [4] D. Mannix, S. Langridge, M. Longfield, W.G. Stirling, G.H. Lander, J. Rebizant, W. Nuttall, C.S., S. Wasserman, L. Soderholm, Phys. Rev. B (in press).
- [5] J.M. Wills, B.R. Cooper, Phys. Rev. B 42 (1990) 4682–4693.
- [6] H. Stragier, J.O. Cross, J.J. Rehr, L.B. Sorensen, C.E. Bouldin, J.C. Woicik, Phys. Rev. Lett. 69 (1992) 3064–3067.
- [7] D.C. Koningsberger, R. Prins (Eds.), X-ray Absorption: Principles, Applications, Techniques of EXAFS, SEXAFS and XANES, John Wiley and Sons, New York, 1988.
- [8] B.K. Teo, EXAFS: Basic Principles and Data Analysis; Springer-Verlag, Berlin, 1986, p. 132.
- [9] O.L. Kruger, J.B. Moser, J. Phys. Chem. Solids 28 (1967) 2321–2325.
- [10] F. Weigel, J.J. Katz, G.T. Seaborg, Plutonium. In: J.J. Katz, G.T. Seaborg, L.R. Morss (Ed.), The Chemistry of the Actinide Elements, Vol. 1, Chap. 7, 2nd ed., Chapman and Hall, London, 1986.
- [11] S.I. Zabinsky, J.J. Rehr, A. Ankudinov, R.C. Albers, M.J. Eller, Phys. Rev. B 52 (1995) 2995–3009.
- [12] J.C. Spirlet, O. Vogt, Sample preparation and crystal growth for solid state actinide research. In: A.J. Freeman, G.H. Lander (Eds.), Handbook on the Physics and Chemistry of the Actinides, Vol. 1, North-Holland, Amsterdam, 1984, pp. 79–151.
- [13] D.T. Larson, J.M. Haschke, Inorg. Chem. 20 (1981) 1945–1950.
- [14] Y. Baskin, S.D. Smith, J. Nucl. Mater. 37 (1970) 209.
- [15] L.R. Morss. In: J.J. Katz, G.T. Seaborg, L.R. Morss (Eds.), Thermodynamic Properties, The Chemistry of the Actinide Elements, Vol. 2, Chap. 17, 2nd ed., Chapman and Hall, London, 1986.
- [16] D.D. Wagman, W.H. Evans, V.B. Parker, H. Schumm, I. Halow, S.M. Bailey, K.L. Churney, R.L. Nuttall, J. Phys. Chem. Ref. Data 11(Suppl. 2) (1982) 2–79.
- [17] G. Kalkowski, G. Kaindl, S. Bertran, G. Schmiester, J. Rebizant, J.C. Spirlet, O. Vogt, Solid State Comm. 64 (1987) 193–196.
- [18] W.H. McMaster, N. Kerr Del Grande, J.H. Mallett, J.H. Hubbell, Compilation of X-ray Cross Sections, Lawrence Radiation Laboratory, Livermore, CA, 1969, UCRL-50174-SEC 2-R-1.